Turning up the HEAT: Surgical simulation of the Moses 2.0 laser in an anatomic model

Christopher Wanderling[1], Aaron Saxton[1], Dennis Phan[1], Karen Doersch[1], Lauren Shepard[2], Nathan Schuler[1], Thomas Osinski[1], Scott Quarrier[1], Ahmed Ghazi[2]
[1]University of Rochester Medical Center, Department of Urology, Rochester, NY, United States; [2]Brady Urologic Institute, Johns Hopkins University, Baltimore, MD, United States

Acknowledgement: *The authors would like to graciously thank Dr. William Roberts from the University of Michigan for providing his expertise, input, and guidance in our project. We largely based our project on the excellent work his lab has produced. He reviewed our data and provided insight for data evaluation to provide impactful results.*

Cite as: Wanderling C, Saxton A, Phan D, et al. Turning up the HEAT: Surgical simulation of the Moses 2.0 laser in an anatomic model. *Can Urol Assoc J* 2024 March 1; Epub ahead of print. http://dx.doi.org/10.5489/cuaj.8673

Published online March 1, 2024

Corresponding author: Dr. Christopher Wanderling, University of Rochester Medical Center, Department of Urology, Rochester, NY, United States; Christopher_Wanderling@URMC.Rochester.edu

***

ABSTRACT

Introduction: With advancements in laser technology, urologists have been able to treat urinary calculi more efficiently by increasing the energy delivered to the stone. With increases in power used, there is an increase in temperatures generated during laser lithotripsy. The aim of this study was to evaluate the thermal dose and temperatures generated with four laser settings at a standardized power in a high-fidelity, anatomic model.

Methods: Using high-fidelity, 3D printed hydrogel models of a pelvicalyceal collecting system with a synthetic BegoStone implanted in the renal pelvis, surgical simulation of ureteroscopic laser lithotripsy was performed with the Moses 2.0 holmium laser. At a standard power (40 W) and irrigation pressure (100 cm H_2O), we evaluated operator duty cycle (ODC) variations with different time-on intervals at four different laser

KEY MESSAGES

- The time to TD_{43} was generally faster at the stone.
- Temperatures and cumulative thermal doses were greater closer to the laser fiber tip.
- Longer laser-on times yielded greater cumulative thermal doses, while shorter laser-off intervals reached the TD_{43} faster.
- ODCs of ≥75% reached the threshold of thermal injury.

settings. Temperature was measured at two separate locations: at the stone and ureteropelvic junction.
Results: Greater cumulative thermal doses and maximal temperatures were achieved with greater ODCs and longer laser activation periods. There were statistically significant differences between the thermal doses and temperature profiles of the laser settings evaluated. Temperatures were greater closer to the tip of the laser fiber.
Conclusions: Laser energy and frequency play an important role in the thermal loads delivered during laser lithotripsy. Urologists must perform laser lithotripsy cautiously when aggressively treating large renal pelvis stones, as dangerous temperatures can be reached. To reduce the risk of causing thermal tissue injury, urologists should consider reducing their ODC and laser-on time.

INTRODUCTION

Advancements in laser technology has allowed urologists to safely treat urolithiasis endoscopically for years. The Holmium: Yttrium-Aluminum-Garnet (Ho:YAG) laser has been accepted as a standard lithotripsy laser due its ability to pulverize stones of many compositions [1]. With the increasing prevalence of high-powered lasers ($\geq$100W), more urologists have been utilizing this technology as the they can deliver energy at higher frequencies (>120Hz) leading to improved stone ablation efficiency and decrease operative time [2]. However, with increased power, there is increased heat generated. With this in mind, it is important to preserve patient safety while determining the most efficient method of stone ablation.

Lasers are able to be utilized for calculus ablation because the stone is able to absorb the emitted laser energy leading to stone fragmentation and melting, thus temperature and thermal dose have been studied extensively. Thermal dose was first described by Sapareto and Dewey; it is the cumulative equivalent minutes, held at $43^{O}C$ (TD_{43}) and is a standard measure for tissue denaturation occurring when $TD_{43} \geq 120$ equivalent minutes [3-5]. Previously this lab, along with others, have attempted to study thermal loads during ureteroscopic (URS) laser lithotripsy.

The majority of these studies have been performed in low-fidelity *in vitro* models consisting of test tubes or syringes or with *ex vivo* porcine kidney models. The weakness of the *in vitro* models is that they may not accurately simulate surgical conditions. Conversely, while *ex vivo* models may be the closest simulation to surgery, animal models encompass financial and ethical dilemmas.

The goal of our study was to improve upon and confirm our prior studies, using a validated high-fidelity anatomic human kidney model [6]. Using image segmentation, 3D printing, and hydrogel casting, a model inclusive of a complete pelvicalyceal collecting system (PCS) with a ureteral access sheath (UAS) simulating the full length ureter and incorporating a 2 cm BegoStone was fabricated. This model was then submerged in water bath maintained at $37^{O}C$.

The aims of this study were:

1. Evaluate the temperature profile of the Moses 2.0 Ho:YAG laser at the stone and UPJ for four different 40W laser settings (two fragmentation and two dusting) using three operator duty cycles (ODCs).
2. Evaluate and compare time to TD_{43} for each laser setting.

METHODS

Simulation model fabrication

Digital Imaging and Communications in Medicine (DICOM) data from a patient's CT scan was segmented into a 3D computer-aided design (CAD) model using Mimics software (Materialize, Leuven, Belgium). The 3D CAD model (including the PCS/ ureter) was 3D printed using hydrogel filament (Fusion3 Design, Greensboro, NC) with a synthetic BegoStone (prepared with 10:1 powder to water ratio by weight) positioned in the renal pelvis and coated with a second polyvinyl alcohol (PVA) mixture (Figure 1A & B). This was then implanted into a hydrogel kidney block. The model was submerged in a warm water bath at anatomic temperature (starting temperature 37.0^{o}C +/- 2.0^{o}C); the water was circulated using a Sou Vide (Anova Applied Electronics, San Fransisco, USA). The final product underwent extensive mechanical and computational fluid dynamic (CFD) testing to replicate PCS properties, stone lithotripsy and fluid flow (Figure 1C & D).

Laser lithotripsy

URS laser lithotripsy was performed at a standardized power (40W, short pulse width, Moses Technology activated) with continuous normal saline irrigation (17.5 ml/min) via retrograde access with a flexible ureteroscope (LithoVue, Boston Scientific) and a 200µm Ho:YAG laser fiber (Moses 2.0, Boston Scientific; Figure 2). A 12/14 Fr, 40cm UAS was inserted just distal to the ureteropelvic junction (UPJ) to simulate a complete ureteral length. Four laser settings - two fragmentation (1J x 40Hz and 2J x 20Hz) and two dusting (0.5J x 80Hz, 0.4J x 100Hz) were tested. We evaluated 3 ODCs (50, 75, and 100%) with different laser-on (30, 60, and 120s) times. Each experiment consisted of 10 cycles (1 cycle = 1 laser-on/ laser-off sequence = 1 ODC); the 100% ODC consisted of pedal-on time of 12min straight with no laser-off time. Five permutations of each laser setting were tested. A total of 20 experiments were performed. Temperature was measured continuously with data analysis performed in 10s intervals.

Data collection and analysis

Temperature was recorded with K-type needle thermocouple probes and data logger (Omega, Norwalk, CT) at two standard positions (registered in the model) in the PCS- at the stone (renal pelvis) and UPJ. Additionally, a third temperature probe was inserted into the hydrogel block. Thermal dose was calculated with the Sapareto and Dewey formula. Statistical analysis for thermal dose was analyzed via area under the curve (AUC) and Kruskal-Wallis comparison and

temperature data was analyzed via non-linear regression in a third-order polynomial (Prism 9). $P<0.05$ was considered statistically significant.

RESULTS

When evaluating the cumulative thermal dose, it was found to be higher *at the stone* than at the UPJ for each laser setting tested. There was a statistically significant difference between cumulative thermal dose at the stone and UPJ for each laser setting tested (Table 1).

The threshold of thermal injury was reached for the 100 and 75% ODCs both at the stone and UPJ but was not reached in any 50% ODC. The threshold of thermal injury was reached faster for 100% ODC than either of the 75% ODC time intervals. For the 75% ODCs, the 30s on/ 10s off time interval reached the threshold faster for all laser settings tested except for 2J x 20Hz where the 60s on/ 20s off interval was faster. The time to reach the threshold of thermal injury was typically faster at the stone compared to the UPJ except for 1J x 40Hz (100% ODC, 30s on/ 10s off) where the UPJ reached the threshold faster while for 2J x 20Hz (30s on/ 10s off) and 0.5J x 80Hz (100% ODC) the threshold was reached at approximately the same time (Table 1).

The cumulative thermal dose was greater for each laser setting with greater ODCs both at the stone and UPJ. 2J x 20Hz delivered the greatest cumulative thermal dose for each time interval tested except for 30s on/ 10s off where it delivered the lowest cumulative thermal dose. There was no other generalizable pattern appreciated between the laser settings otherwise when compared against one another (Table 1 and 2).

Considering maximal temperatures at the stone vs. UPJ, the temperatures were higher at the stone in 13/20 tests, higher at the UPJ in 6/20 tests and once test the maximal temperature was the same (2J x 20Hz, 30s on/ 10s off). There was a statistically significant difference in the temperature curves for all but 3 tests (1J x 40Hz- 60s on/ 20s off and 60s on/ 60s off, 2J x 20Hz, 30s on/ 30s off). Temperatures were hotter with greater ODCs for each laser setting both at the stone and at the UPJ. Considering the 75% ODCs, hotter maximal temperatures were recorded with a longer laser-on time (60s on/ 20s off) for each laser setting both at the stone and at the UPJ. Considering the 50% ODCs, there were mixed results as to which laser time-on cycle generated hotter maximal temperatures; for the fragmentation settings, the 30s on/ 30s off cycle yielded hotter temperatures while for the dusting settings, the 60s on/ 60s off cycle was hotter. This held true both at the stone and at the UPJ (Table 2).

While there was not an apparent trend as to which laser setting produced the hottest temperatures, we did appreciate statistically significant differences between laser settings which demonstrates that frequency and energy can strongly influence temperature and thermal dose, even at a standardized power. For 100% ODC, 2J x 20Hz was hottest at the stone and UPJ while 0.4J x 100Hz was the lowest for both. For the other 4 ODC/ time-on intervals evaluated, there was no overall trend (Table 1 and 2).

Temperatures of the hydrogel block started at $37.0^{O}C$ +/- $2.1^{O}C$ and increased $1.0^{O}C$ +/- $2.0^{O}C$. There were no statistically significant changes in temperature measured at this location. It was observed that the temperatures increased slightly more when the starting temperature was

lower (<37^{O}C) opposed to a minimal temperature fluctuation at higher starting temperatures (≥ 37^{O}C).

DISCUSSION

In this study, we were able to establish that temperatures and cumulative thermal doses were greater closer to the tip of the last fiber which has also been recognized in previous studies [7]. Additionally, we demonstrated that energy and frequency play a significant role in the thermal load delivered and the previously accepted concept that power is the sole determinant of temperature may not be entirely accurate [5, 8-10]. In general, greater thermal doses and maximal temperatures were achieved with greater ODCs and longer laser-on times for 100% and 75% ODCs, which is in agreement with previously published literature [11, 12]. When comparing laser-on times for 75% ODC, 60s on/ 20s off delivered greater cumulative thermal doses and maximal temperatures for each laser setting both at the stone and UPJ.

Interestingly, when evaluating 50% ODCs, the fragmentation settings delivered greater cumulative thermal doses for shorter laser-on time (30s on/ 30s off) while the dusting settings delivered greater cumulative thermal doses for the longer laser-on time (60s on/ 60s off). When considering maximal temperatures, the same results held true except for 1J x 40Hz at the UPJ (43.1^{O}C for 30s on/ 30s off vs. 43.3^{O}C for 60s on/ 60s off). This shows that the laser-off time may play a crucial role in fluid cool-down as the longer the laser is off, the greater the opportunity that the fresh irrigation inflow can cool more of the PCS.

There have been numerous studies manipulating variables involved during URS laser lithotripsy. Dr. William Robert's Lab at the University of Michigan has led many studies via *in vitro* bench models and computational modelling. They have evaluated the Ho:YAG laser power (2.5-50W), frequency (5-80Hz), irrigation rate (0-40ml/min), irrigation temperature (~0^{O}C and 19^{O}C), and ODC (≥50%) [4, 5, 11-14]. Their work sought to adapt their previous findings to an *in vivo* porcine model and found that temperatures capable of tissue damage were easily achieved but can be negated by increasing irrigation flow rate [15]. Other labs have also evaluated irrigation rates and have determined that increased irrigation rates can mitigate temperature increases during active lasing, as too can the use of a UAS [16-18].

A recent study evaluated intraoperative irrigation fluid temperatures during URS treatment of urolithiasis. They compared laser settings of 1J x 20Hz and 0.5J x 20Hz with irrigation rates of 0ml/min, 15ml/min, and 30ml/min. They found that with irrigation rates of 15ml/min and 30ml/min a temperature of 43^{O}C was not reached after 60s straight of laser activation. [19]. Our study utilized a UAS with a constant irrigation flow (100cm H_2O = 17.5 ml/min). We found that at a constant power, the threshold of thermal injury could be reached in as little as 195s (2J x 20Hz, at the stone and 1J x 40Hz, at the UPJ). While there was a significant difference in power tested between Teng, et. al's study and ours, it is obvious that when treating larger stone burdens, urologists must be diligent when continuously lasing as temperatures can reach dangerous levels, even with UAS use.

It is important to consider that in this study, we were lasing a large calculus in the renal pelvis where there is more volume/ area for fluid and irrigation flow. Previous studies have demonstrated that when lasing in smaller spaces, temperatures increased faster and the threshold of thermal injury could be reached faster when compared to larger spaces [20, 21]. In agreement with our prior evaluations and previous studies, the threshold of thermal injury was reached during ODCs greater than 70% [11]. This held true regardless the laser settings tested and for laser-on time. Aldoukhi, et. al. performed a chart review of 63 URS cases and determined that during the 60 seconds of greatest power delivered, the ODC was 63% [12].

Although studies have demonstrated that ODCs <70% are less likely to cross the threshold of thermal injury, it is important to consider that more powerful laser settings can deliver greater thermal loads in shorter amounts of time and with shorter ODCs. Additionally, when lasing in tighter spaces, such as a calyx opposed to the renal pelvis, it is reasonable to believe that the threshold of thermal injury could be reached even with lower ODCs or less powerful laser settings, particularly after a stone is broken as the laser tip may be closer to the urothelium with no interruption from a stone and it is not absorbing energy once pulverized. In an *in vitro* model, it was found that the presence of a phantom BegoStone was related to lower rises in fluid temperatures when compared with no stone was present at an array of powers tested (10, 20, 40, 60W) [20].

It is recognized that BegoStones may possess distinctive photothermal properties compared with real urolithiasis during laser lithotripsy [22]. However, BegoStones are often accepted as a synthetic analogue for real urolithiasis during *in vitro* urologic laser studies since they are able to be composed without significant difficulty in an efficacious manner and are able to be fabricated and reproduced with the same composition.

To date, this appears to be the first study evaluating thermal loads performed in a high-fidelity anatomic *in vitro* model at anatomic temperature WITH a UAS utilized while actively lasing a phantom stone. Other studies have been performed utilizing *ex vivo* and *in vivo* models with or without UAS that can simulate the complete ureteral length. It is well-recognized that using a UAS can facilitate higher irrigation flow rates and modulate temperature increases easier, in addition to reducing intrarenal pressures during irrigation [17, 23].

With regards to the power setting evaluated utilizing the Moses 2.0 Ho:YAG laser in this study, 40W was chosen as the standard because this power allowed for the variation of both frequency and energy settings for four different laser settings- two dusting and two fragmentation, while maintaining the constant power. It is recognized that urologists may commonly utilize lower power settings in clinical practice, however, the goal of this study was evaluate variables besides power since many previous studies have already compared different power settings [4, 5, 13].

This study addressed some of the limitations of our previous studies which had been performed at room temperature. With this experimental model, we evaluated thermal dose and temperatures in the high-fidelity anatomic model performed at anatomic temperature with a

UAS. This experimental design appears to be a quality, realistic *in vitro* model for URS laser lithotripsy. The majority of previous studies have been performed with *in vitro* test tube models or with *ex vivo* porcine kidney models.

While we have addressed some limitations of our prior studies, we recognize that some limitations are present. First, although this project was performed in a high-fidelity anatomic PCS model, some caution should be maintained when attempting to correlate this data to a surgical scenario. Second, only one PCS model was utilized in our evaluations in efforts to further reduce confounding variables influencing our results. Finally, although BegoStone models may simulate actual kidney stones, they may not act as an exact analogue. Our lab hopes to continue pursuing urologic laser research in the future, building on this study, and addressing some of these limitations.

This study had several strengths. First, this study evaluated four variables: laser frequency, laser energy, ODC, and laser time-on, in an anatomically correct, high-fidelity model that has been validated with mechanical and CFD testing but this time AT anatomic temperature with the use of a UAS. Second, we were able to evaluate thermal load in two locations in the PCS. Finally, we were able to measure the temperatures while actively lasing a synthetic 2cm calculus. The combination of these components into one model while analyzing four separate variables strengthens the results of this study. While prior studies have compared some of these factors affecting irrigation fluid temperature, the majority of these studies focus on fewer variables.

CONCLUSIONS

We were able to validate our previous studies and address several limitations with this experimental model. We confirmed that dangerous thermal loads can be delivered with greater ODCs and longer laser-on times. We demonstrated again that at a standardized power, energy and frequency manipulations can strongly influence thermal dose and temperatures. Based on the results of this study, it is important that urologists perform URS laser lithotripsy diligently as irrigation fluid temperatures and cumulative thermal doses in the PCS can reach critical levels and potentially cause urothelial injury, regardless of laser setting.

REFERENCES

1. Kronenberg P, and Somani B. Advances in lasers for the treatment of stones-a systematic review. *Curr Urol Rep* 2018;19:45. https://doi.org/10.1007/s11934-018-0807-y
2. Dauw, C.A., et al. Contemporary practice patterns of flexible ureteroscopy for treating renal stones: Results of a worldwide survey. *J Endourol* 2015;29:1221-30. https://doi.org/10.1089/end.2015.0260
3. Sapareto, SA, Dewey WC. Thermal dose determination in cancer therapy. *Int J Radiat Oncol Biol Phys* 1984;10:787-800. https://doi.org/10.1016/0360-3016(84)90379-1
4. Maxwell, A.D., et al. Simulation of laser lithotripsy-induced heating in the urinary tract. *J Endourol* 2019;33:113-9. https://doi.org/10.1089/end.2018.0485
5. Aldoukhi, A.H., et al. thermal response to high-power holmium laser lithotripsy. *J Endourol* 2017;31:1308-12. https://doi.org/10.1089/end.2017.0679
6. Saba P, Belfast E, Melnyk R, et al. Development of a high-fidelity robot-assisted kidney transplant simulation platform using three-dimensional printing and hydrogel casting technologies. *J Endourol* 2020;34:1088-94. https://doi.org/10.1089/end.2020.0441
7. Taratkin M, Laukhtina E, Singla N, et al. Temperature changes during laser lithotripsy with Ho:YAG laser and novel Tm-fiber laser: A comparative in-vitro study. *World J Urol* 2020;38:3261-6. https://doi.org/10.1007/s00345-020-03122-1
8. De Coninck V, Defraigne C, Traxer O. Watt determines the temperature during laser lithotripsy. *World J Urol* 2022;40:1257-8.
9. Petzold R, Suarez-Ibarrola R, Miernik A. temperature assessment of a novel pulsed thulium solid-state laser compared with a holmium:yttrium-aluminum-garnet laser. *J Endourol* 2021;35:853-9. https://doi.org/10.1089/end.2020.0803
10. Molina WR, Carrera RV, Chew BH, et al. Temperature rise during ureteral laser lithotripsy: Comparison of super pulse thulium fiber laser (SPTF) vs high power 120 W holmium-YAG laser (Ho:YAG). *World J Urol* 2021;39:3951-6. https://doi.org/10.1007/s00345-021-03619-3
11. Louters MM, Dau JJ, Hall TL, et al. Laser operator duty cycle effect on temperature and thermal dose: in-vitro study. *World J Urol* 2022;40:1575-80. https://doi.org/10.1007/s00345-022-03967-8
12. Aldoukhi AH, Dau JJ, Majdalany SE, et al. Patterns of laser activation during ureteroscopic lithotripsy: Effects on caliceal fluid temperature and thermal dose. *J Endourol* 2021;35:1217-22. https://doi.org/10.1089/end.2020.1067
13. Aldoukhi AH, Black KM, Hall TL, et al. Defining thermally safe laser lithotripsy power and irrigation parameters: In vitro model. *J Endourol* 2020;34:76-81. https://doi.org/10.1089/end.2019.0499
14. Dau JJ, Hall TL, Maxwell AD, et al. Effect of chilled irrigation on caliceal fluid temperature and time to thermal injury threshold during laser lithotripsy: In vitro model. *J Endourol* 2021;35:700-5. https://doi.org/10.1089/end.2020.0896
15. Aldoukhi AH, Hall TL, Ghani KR, et al. Caliceal fluid temperature during high-power holmium laser lithotripsy in an in vivo porcine model. *J Endourol* 2018;32:724-9. https://doi.org/10.1089/end.2018.0395
16. Tsaturyan A, Peteinaris A, Pantazis L, et al. The effect of prolonged laser activation on irrigation fluid temperature: an in vitro experimental study. *World J Urol* 2022;40:1873-8. https://doi.org/10.1007/s00345-022-04000-8

17. Gallegos H, Bravo JC, Sepúlveda F, et al. Intrarenal temperature measurement associated with holmium laser intracorporeal lithotripsy in an ex vivo model. *Cent European J Urol* 2021;74:588-94. https://doi.org/10.5173/ceju.2021.0092
18. Wriedt R, Yilmaz M, Lottner T, et al. Assessing critical temperature dose areas in the kidney by magnetic resonance imaging thermometry in an ex vivo Holmium:YAG laser lithotripsy model. *World J Urol* 2023;41:543-9. https://doi.org/10.1007/s00345-022-04255-1
19. Teng J, Wang Y, Jia Z, et al. Temperature profiles of calyceal irrigation fluids during flexible ureteroscopic Ho:YAG laser lithotripsy. *Int Urol Nephrol* 2021;53:415-9. https://doi.org/10.1007/s11255-020-02665-x
20. Peteinaris A, Tsaturyan A, Pantazis L, et al. Factors affecting the irrigation fluid temperature during laser lithotripsy: In vitro experimental study. *Urology* 2022;170:53-9. https://doi.org/10.1016/j.urology.2022.07.060
21. Rezakahn Khajeh N, Hall TL, et al. Pelvicaliceal volume and fluid temperature elevation during laser lithotripsy. *J Endourol* 2022;36:22-8. https://doi.org/10.1089/end.2021.0383
22. King JB, Katta N, Teichman JMH, et al. Mechanisms of pulse modulated holmium:YAG lithotripsy. *J Endourol* 2021;35:S29-36. https://doi.org/10.1089/end.2021.0742
23. Peteinaris A, Pagonis K, Vagionis A, et al. What is the impact of pulse modulation technology, laser settings and intraoperative irrigation conditions on the irrigation fluid temperature during flexible ureteroscopy? An in vivo experiment using artificial stones. *World J Urol* 2022;40:1853-8. https://doi.org/10.1007/s00345-022-04002-6

FIGURES AND TABLES

Figure 1. (A) 3D printed PVA PCS model with embedded BegoStone before coating with hydrogel. (B) Final hydrogel PCS model with drainage tubing secured acting as UPJ (stone inside model, unable to be visualized). (C & D) CFD testing of the model at 100cm H_2O

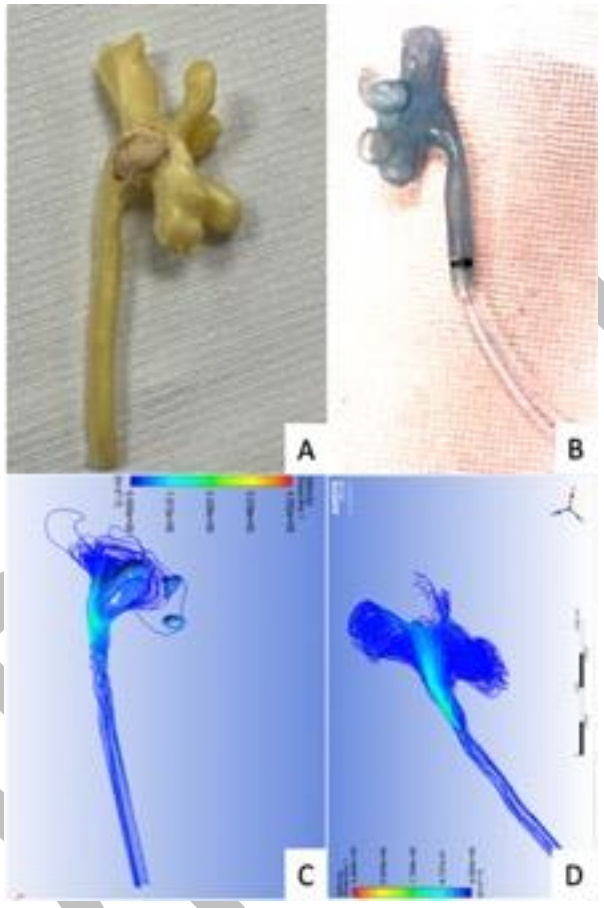

Figure 2. Temperature and thermal dose graphs of each laser setting at the stone. TD_{43} (solid red line) is on the thermal dose graphs. 100% ODC (A) thermal dose; (B) temperature. 75% ODC: 30s on/10s off; (C) thermal dose and (D) temperature 60s on/20s off; (E) thermal dose and (F) temperature 50% ODC: 30s on/30s off; (G) thermal dose and (H) temperature 60s on/60s off; (I) thermal dose and (J) temperature.

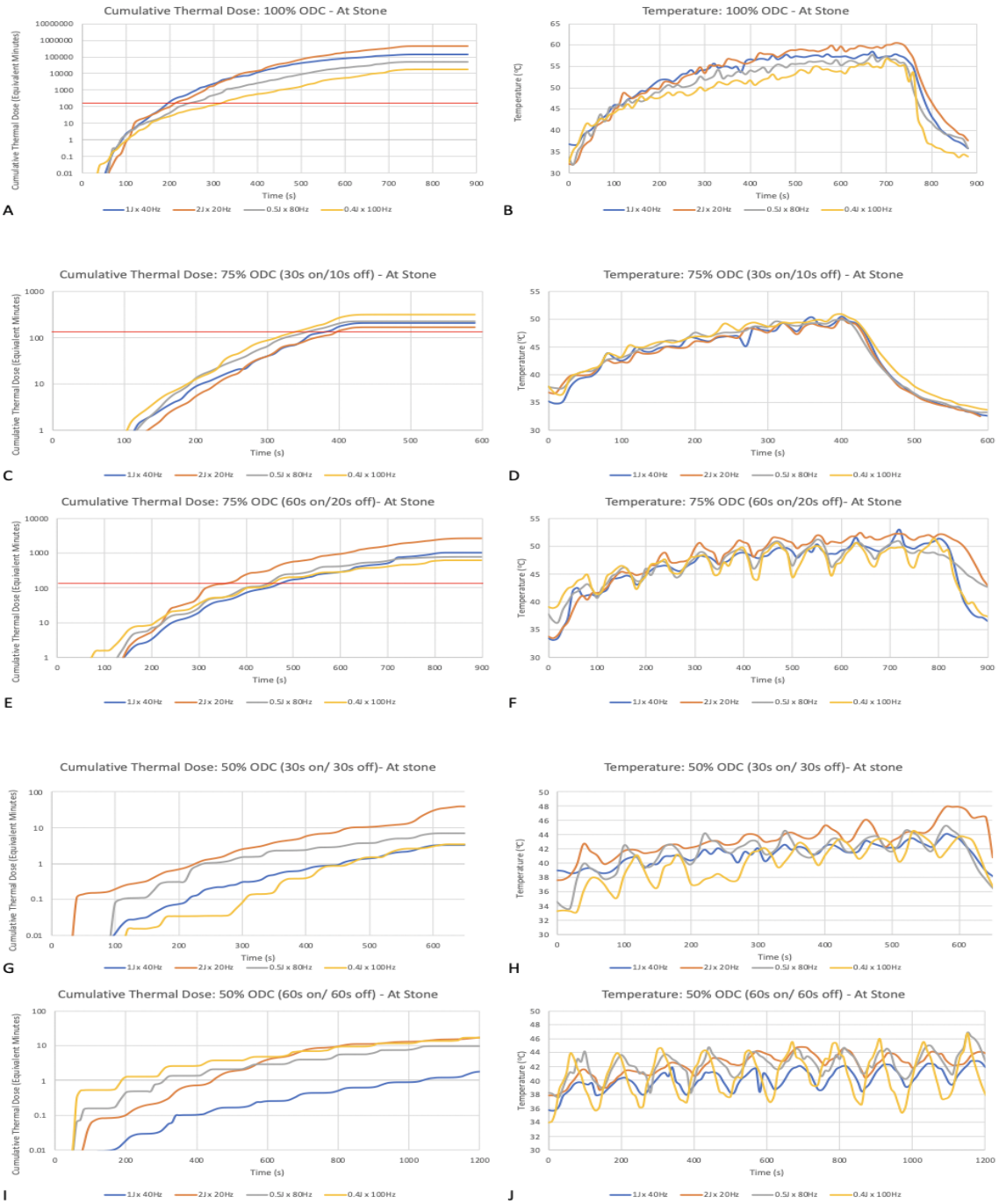

Table 1. Comparison of cumulative thermal dose, time to TD_{43}, and statistical comparison at the stone vs. UPJ

Laser setting	ODC	Time on (s)/ time off (s)	Cumulative thermal dose (CEM)		Time to thermal injury threshold (s)		p at vs. away from stone
			At stone	Away from stone	At stone	Away from stone	
1 J x 40 Hz	100%		93909.8907	134501.2717	200	195	<0.0001
	75%	30/10	221.6387713	206.1101383	380	370	<0.0001
		60/20	1125.62778	1025.910058	440	465	<0.0001
	50%	30/30	3.569467179	3.071237613	NR	NR	<0.0001
		60/60	3.233970832	1.882688132	NR	NR	<0.0001
2 J x 20 Hz	100%		318276.667	449089.338	195	205	<0.0001
	75%	30/10	187.32621	169.9063665	395	395	0.0004
		60/20	3398.569694	2690.290273	325	330	<0.0001
	50%	30/30	51.75861439	39.50125173	NR	NR	<0.0001
		60/60	24.86021107	18.09596256	NR	NR	<0.0001
0.5 J x 80 Hz	100%		62134.7335	51936.32456	230	230	<0.0001
	75%	30/10	344.6057609	228.1060048	320	350	<0.0001
		60/20	1253.588927	788.0238063	395	435	<0.0001
	50%	30/30	11.20336357	7.050187058	NR	NR	<0.0001
		60/60	23.62071365	9.677738417	NR	NR	<0.0001
0.4 J x 100 Hz	100%		18045.01532	8502.241086	295	315	<0.0001
	75%	30/10	316.2694821	242.2321829	330	380	<0.0001
		60/20	739.8320632	627.1075826	410	450	<0.0001
	50%	30/30	3.071237613	3.569467179	NR	NR	<0.0001
		60/60	18.93383935	17.0028632	NR	NR	<0.0001

Highlighted cells indicate test that exceeded threshold of thermal injury. NR indicates that the threshold of thermal injury was not reached. Statistics comparing cumulative thermal dose and calculated with Kruskal-Wallis.

Table 2. Comparison of maximal temperature, and statistical comparison at the stone vs. UPJ					
Laser setting	**ODC**	**Time on (s)/ time off (s)**	**Maximum temperature (*C)**		**p at vs. away from stone**
			At stone	**Away from stone**	
1 J x 40 Hz	100%		58.5	58.2	<0.0001
	75%	30/10	50.4	50.2	<0.0001
		60/20	52.9	51.6	0.1618
	50%	30/30	44.1	43.1	0.0018
		60/60	42.8	43.3	0.1187
2 J x 20 Hz	100%		60.5	59.9	<0.0001
	75%	30/10	50.1	50.1	<0.0001
		60/20	52.4	52.7	0.0224
	50%	30/30	47.9	48.8	0.1638
		60/60	44.8	45.3	0.0301
0.5 J x 80 Hz	100%		57.8	57.6	<0.0001
	75%	30/10	49.9	50.8	<0.0001
		60/20	51.2	52.1	0.0014
	50%	30/30	45.2	44.4	<0.0001
		60/60	46.9	45.1	<0.0001
0.4 J x 100 Hz	100%		56.7	55.3	<0.0001
	75%	30/10	50.8	49.9	<0.0001
		60/20	51.4	51.0	<0.0001
	50%	30/30	44.4	43.8	<0.0001
		60/60	46.7	45.2	<0.0001

Highlighted cells indicate test that exceeded threshold of thermal injury. Statistics comparing temperature curves and calculated with non-linear regression in a third-order polynomial.